Journal of Information Systems Engineering and Management
2025, 10(7s)
e-ISSN: 2468-4376
https://www.jisem-journal.com/

Research Article

A Miniaturized Multiband Antenna with Frequency Reconfiguration for 5G and IoT Applications

Dr. Koduri Sreelakshmi[1], Biswa Ranjan Swain[2], Amiya Bhusana Sahoo[3], Manas Ranjan Jena[4], Rajiv Pathak[5]
[1]*Department of Electronics and Communication Engineering, Baba institute of technology & Sciences (A), Vishakhapatnam, India*
[2]*Department of Electronics and Telecommunication Engineering, Veer Surendra Sai University of Technology, Burla, Odisha, India*
[3]*Department of Electronics and Communication Engineering, Silicon University, Bhubaneswar, Odisha, India*
[4]*Department of Electronics and Communication Engineering, Silicon Institute of Technology, Sambalpur, Odisha, India*
[5]*Department of Information Technology, Bhilai Institute of Technology, Durg, Chhattisgarh, India*

ARTICLE INFO

Received: 14Oct 2024

Revised: 07Dec 2024

Accepted: 23Dec 2024

ABSTRACT

This research focuses on designing and testing a compact, multiband antenna that can switch between different frequency bands using a PIN diode. The demonstrated antenna is constructed on a 1.6 mm thick FR4 substrate and features a ground plane on the rear side. Because of its small dimensions (24 mm x 19 mm × 1.6 mm), it can be effortlessly incorporated into various kinds of RF front-end systems. The antenna presented is capable of achieving hexa/Triple band characteristics through the utilization of a PIN diode positioned between the metal strip and the F shaped monopole. The examined antenna is capable of operating in L and C bands across a range of six different frequencies when the PIN diode is inactive: 2.54 GHz, 2.64 GHz, 3.48 GHz, 4.3 GHz, 5.25 GHz, and 5.68 GHz supporting 5G and IOT services. Conversely, with the PIN diode activated, it functions in C-band across three specific frequencies: 4.3 GHz, 5.2 GHz, and 5.68 GHz supporting IOT services. The investigated antenna exhibits very small frequency ratios between two consecutive bands of the value of 1.04/1.3/1.23/1.22/1.08, respectively. The investigated design is fabricated and results of the design under investigation were compared, showing a strong correlation between the simulated and measured data.

Keywords: Hexaband, IOT, PIN Diode, Reconfigurable, 5G.

INTRODUCTION

With the continuous progress of wireless communication technology, current transceiver systems offer a wide range of services including multimedia streaming, data transmission, GPS, telephony, Bluetooth connectivity and internet access. However, antennas intended to operate in a single frequency band [1] are limited to supporting only one service, restricting their versatility in multifunctional applications. Multiple-radio applications frequently require several antennas, which can lead to size, interference, and cost issues. Compact multiband antennas provide a solution by integrating many frequency bands into a single, smaller antenna, minimizing the overall system size and making installation easier. Although ultra-wideband or broadband antennas can handle several frequency bands, they may not be suitable for situations where specific frequencies must be eliminated to minimize interference. In these instances, multiband antennas are required to selectively transmit and receive signals while reducing interference. Numerous researchers have attempted to develop such antennas that are suitable for multiband operations [2]. Designing multiband antennas demands thorough investigation of the frequency ratio between resonance bands. Smaller frequency ratio decreases wasted bandwidth and interference between bands, enhancing overall system performance. Numerous antenna configurations with a small frequency ratio have been proposed [3–6]. A novel multiband unidirectional patch antenna with integrated resonators is investigated in [7]. The rectangular slotted patch antenna described in [8] is designed to operate in five different frequency bands. The report in [9] discusses a compact nested rectangular loop penta resonant antenna that is fed with coplanar waveguide. A hexa-band patch antenna with novel design is proposed in [10]. However, there are certain limitations associated with multiband antennas that have small frequency ratios that have been discussed in references [3-10]. Nevertheless, these multiband antennas [3-10] transmit all resonances irrespective of customer requirement, implying that they

are not reconfigurable. Conventional multiband antennas lack frequency-tuning capability. However, frequency reconfigurable antennas provide a solution by allowing for dynamic variation of operating frequencies. This function also helps to decrease out-of-band interference, decreasing the need for complicated front-end filters [11]. Researchers have worked hard to develop frequency reconfigurable antennas for a variety of applications [12-13]. A multiband antenna with the compact size of 50 × 45 × 1.6 mm3 is investigated in [14], and in [15], a printed antenna with the capability of reconfiguring its frequency and pattern is introduced. A compact, inexpensive, low-profile, and simple to integrate frequency reconfigurable antenna system is suggested in [16] and in [17], researchers investigated a compact quad-band frequency reconfigurable antenna. A compact frequency-reconfigurable antenna that employs two PIN diodes to switch across various operating modes is proposed in [18]. A compact, reconfigurable patch antenna for S- and C-band operation, meeting the increased need for wireless applications in these frequency bands is proposed in [19]. However, these antennas [13-19] are reconfigurable, but their large size and restricted range of operating bands make them unsuitable for use in modern RF front-ends with limited antenna area. Additionally, a few of these antennas [13–19] incorporated several bias lines, additional PIN diodes, and lumped components to adjust the operating modes, which added complexity to the antenna design and led to integration and cost challenges.

This study investigates a miniaturized frequency reconfigurable multiband antenna with a grounded asymmetric coplanar strip (GACS) as its feeding structure. The proposed design enables frequency band reconfigurability through the integration of a PIN diode switching device between the rectangular metal strip and the F-shaped monopole. The presented antenna is compatible with different wireless standards, including 5G and IOT services. The paper is structured as follows: Section II discusses the core operating principles, the detailed design approach, and the development process. Section III discusses the PIN diode's biasing circuit and electrical model, which are used to enable frequency reconfiguration. Section IV describes the antenna prototype, as well as measurement and simulation findings for gain, reflection coefficient, efficiency and radiation patterns. Finally, Section V presents a summary of major findings.

II. DESIGN AND CONFIGURATION METHODOLOGY FOR ANTENNA

A. ANTENNA SHAPE AND DIMENSIONS

Figures 1(a) and 1(b) show the top and side configurations of the frequency-reconfigurable multiband antenna, which is built on a 1.6 mm-thick FR4 substrate with a relative permittivity of 4.4 and a loss tangent of 0.024. The investigated antenna measures 24 mm × 19 mm × 1.6 mm and is powered by a 50-ohm GACS feedline. The antenna core consists of a rectangular microstrip patch with trimmed edges and a U-shaped slot. To accomplish frequency reconfigurability, the patch incorporates several monopoles (two T-shaped, inverted L-shaped, F-shaped, and Z-shaped), as well as a PIN diode between the F-shaped monopole and a metal strip, characterized by dimensions T (length) and H (width). The design and optimization of the antenna were performed using high-frequency structure simulation software (HFSS). Detailed dimensions are provided in Table 1

Table I The Investigated Antenna's Precise Dimensions

Attribute	Dimension (mm)	Attribute	Dimension (mm)
Ts	24	Hp	14
Hs	19	c	2
Rx	5.8	d	7
Ry	9.5	b	1.97
Tf	9	a	1.63
Hf	1.1	T1	13.05
e	0.3	T2	2
Tp	10	T3	2.5
T4	5.5	T7	1.7
T5	12.61	T8	8.2
T6	0.3	T9	1
T10	5.1	T11	4.5
T12	12.2	T	12
H	1.5		

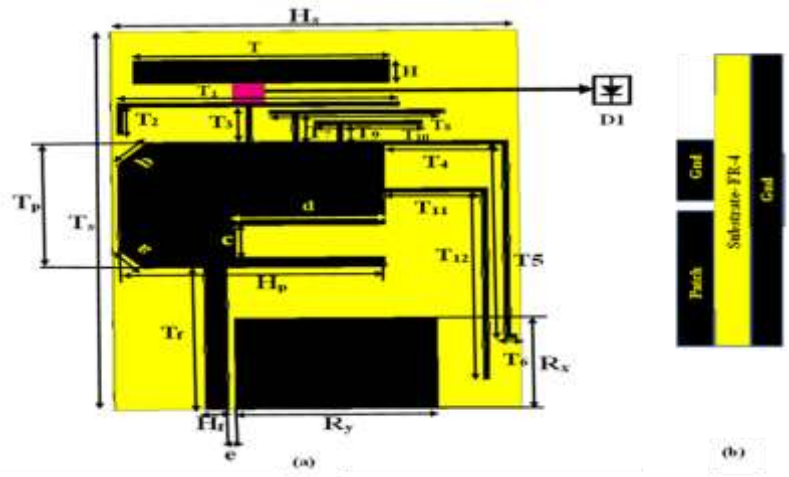

FIGURE 1. Antenna Configuration: a) Front and b) Side Perspectives

B. DESIGN EVOLUTION

Figure 2 depicts each of the design steps, beginning with an elementary rectangular microstrip patch antenna connected to a GACS feedline. To improve impedance matching, edge trimming and a U-shaped slot are included in the patch geometry. This initial design, Antenna I, is optimized for a primary resonance frequency of 5.68 GHz (f_{IOT1}) for IOT applications.

The width (Hp) of Antenna I is derived from Equation (1)

$$H_p = \frac{c}{2f_{IOT1}}\sqrt{\frac{2}{\varepsilon_r+1}} \qquad (1)$$

where c is the speed of light in a vacuum, εr is the dielectric constant of the substrate, and f_{IOT1} is the desired resonant frequency.

The Length (Tp) of Antenna I is derived from Equation (2)

$$T_p = \frac{c}{2f_{IOT1}\sqrt{\varepsilon_{reff}}} - 2\Delta L \qquad (2)$$

where ε_{reff} denotes the effective permittivity, given by Equation (3)

$$\varepsilon_{reff} = \frac{\varepsilon_r+1}{2} + \frac{\varepsilon_r-1}{2\sqrt{1+\frac{12h}{H_p}}} \qquad (3)$$

and ΔL is given by Equation (4)

$$\Delta L = 0.412h\frac{(\varepsilon_{reff}+0.3)\left(\frac{H_p}{h}+0.264\right)}{(\varepsilon_{reff}-0.258)\left(\frac{H_p}{h}+0.8\right)} \qquad (4)$$

where h represents the thickness of substrate

FIGURE 2. Evolution stages of the investigated design

To enable 5G NR n48, an F-shaped monopole is added to Antenna I, resulting in Antenna II. This upgrade allows operation at 3.45 GHz, in addition to the original 5.68 GHz. For the 5G NR n7 uplink, a Z-shaped monopole is inserted

into Antenna II to produce Antenna III, which operates at 2.55 GHz, 3.56 GHz, and 5.68 GHz. To accommodate IoT applications, a T-shaped monopole is added to Antenna III, resulting in Antenna IV, which operates at 2.53 GHz, 3.5 GHz, 4.3 GHz, and 5.68 GHz. Finally, a shorter T-shaped monopole is added to Antenna IV for IOT applications, resulting in Antenna V, which can operate at 2.52 GHz, 3.58 GHz, 4.3 GHz, 5.3 GHz, and 5.68 GHz. Figure 3 shows the reflection coefficient responses for each antenna design. Antenna VI upgrades Antenna V with an inverted L-shaped monopole, allowing it to operate at 2.65 GHz for 5G NR n7 downlink." This final design operates at six frequencies: 2.54 GHz, 2.65 GHz, 3.53 GHz, 4.35 GHz, 5.28 GHz, and 5.68 GHz, with frequency ratios of 1.04/1.3/1.23/1.22/1.08, which are near to one between consecutive resonant frequencies, as shown in Figure 3 and Table 2. The Widths of all the monopoles is taken as 0.3 mm and the lengths of the monopoles in Antennas II–VI are determined as follows:

$$Q2.53\ \text{GHz} = 18.11\ \text{mm}\ (T4+T5+T6) \quad (5)$$

$$Q2.65\ \text{GHz} = 16.7\ \text{mm}\ (T11+T12) \quad (6)$$

$$Q3.45\ \text{GHz} = 17.5\ \text{mm}\ (T1+T2+T3) \quad (7)$$

$$Q4.3\ \text{GHz} = 9.9\ \text{mm}\ (T7+T8) \quad (8)$$

$$Q5.3\ \text{GHz} = 6.1\ \text{mm}\ (T9+T10) \quad (9)$$

These lengths Eq (5-9) are about a quarter of the guided wavelength given by Equation (10)

$$Q_{f_r} = \frac{c}{4f_r\sqrt{\varepsilon_{reff}}} \quad (10)$$

where fr denotes the resonance frequency, c represents the speed of light in vacuum, and εreff signifies the effective permittivity of the substrate, determined by Equation (11)

$$\varepsilon_{reff} = \frac{\varepsilon_r + 1}{2} \quad (11)$$

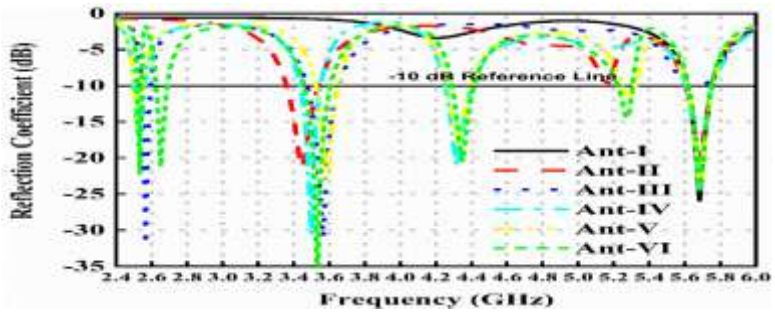

FIGURE 3. Simulated S11 at every stage of evolution

TABLE II

Configuration	Operating frequency (GHz)	S11 (dB)	Bandwidth (GHz)	Bandwidth (MHz)	Gain (dBi)
Antenna-I	5.68	-25.9	5.6-5.76	160	1.7
Antenna-II	3.45	-21.27	3.35-3.54	190	1.2
	5.68	-20	5.6-5.76	160	2.5
Antenna-III	2.56	-31.9	2.54-2.6	60	1.47
	3.56	-31	3.47-3.65	180	2.6
	5.68	-10.3	5.64-5.71	70	4.8
Antenna-IV	2.53	-17.9	2.5-2.56	60	1.5
	3.5	-30.5	3.44-3.55	110	2.0
	4.3	-21	4.25-4.4	150	2.9
	5.68	-24.5	5.61-5.76	120	4.6
Antenna-V	2.52	-15.6	2.5-2.55	50	1.6
	3.58	-22.8	3.53-3.65	120	1.9
	4.3	-18.4	4.26-4.39	130	2.84
	5.3	-11.7	5.25-5.32	70	4.2

	5.68	-24.9	5.61-5.76	150	4.9
Antenna-VI	2.54	-22	2.51-2.57	60	1.6
	2.65	-21.3	2.62-2.69	70	1.9
	3.53	-38.1	3.46-3.61	150	2.84
	4.35	-20.5	4.28-4.4	120	4.2
	5.28	-14.5	5.22-5.31	90	4.9

Simulation-based assessment of the proposed antenna's performance

III. FREQUENCY RECONFIGURABILITY

A. PIN diode model

The proposed design reconfigurability is based on PIN diodes, which were chosen for their desirable qualities such as durability, compact size, quick switching speeds, low capacitance, and manageable resistance in both conducting and non-conducting states. Figure 4(a) depicts the equivalent circuit models for the PIN diode in both operating states. The intrinsic package inductance (L) effects both states. When the diode conducts, the circuit has a relatively low resistance (R_S), which adds to signal loss. In contrast, the non-conducting condition maximizes isolation by using a parallel combination of reverse bias resistance (Rp) and total capacitance (C_T). To provide frequency reconfigurability, the design includes Skyworks Solutions Inc.'s SMP 1320-079 LF PIN diode. The device datasheet specifies the following critical circuit parameters for this diode: L = 0.7 nH, R_S = 0.9 Ω, C_T = 0.3 pF, and Rp = 3 KΩ. In the HFSS simulation, the diode is represented using the Resistance, Inductance, and Capacitance (RLC) boundary, which involves the addition of two rectangular sheets, as shown in Fig. 4(b)

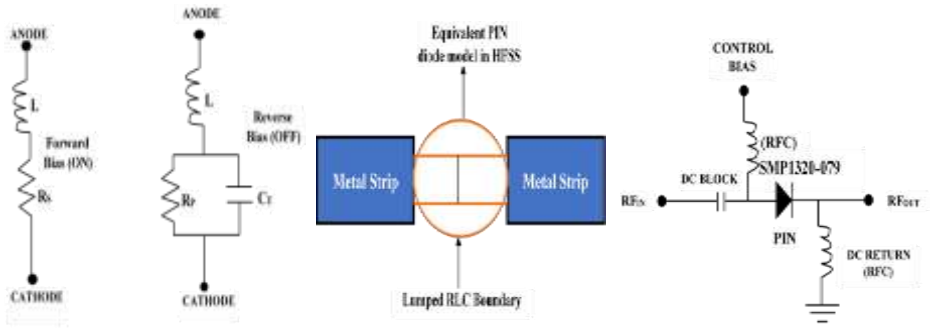

FIGURE 4. PIN diode electrical model a) Equivalent Circuit Using Lumped Elements. b) Model Implementation in HFSS and c) Biasing Circuit Design

B. Biasing circuit

To make sure that the PIN diode is effectively biased, adequate isolation between the DC and RF signals must be maintained. Without proper isolation, RF current can enter the power supply's output impedance, lowering overall efficiency. Figure 4(c) shows how to disconnect the DC bias source from the RF circuit. This is accomplished by connecting a Coil craft 33 nH HF inductor in series with the bias line and a Murata 10 pF RF bypass capacitor in series with the RF input, as shown in Fig. 4(c). Furthermore, the schematic shows how the circuit interfaces to a 5V regulated power source.

IV. RESULTS AND DISCUSSION

A prototype of the proposed antenna along with biasing circuit were built to confirm the HFSS simulation results as shown in Figure 5. The reflection coefficient was determined using a calibrated Agilent/HP N9923A 6 GHz Vector Network Analyzer. This antenna may operate in dual modes with a single PIN diode (D1).

A. Reflection Coefficient

a. MODE 1

In Mode 1, the proposed antenna operates when the PIN diode (D1) is switched off. Figure 6 shows the antenna's S11 parameters in this mode, which indicate impedance bandwidths of roughly 2.52 GHz (2.51-2.53 GHz), 2.63 GHz (2.62-2.67 GHz), 3.48 GHz (3.4-3.56 GHz), 4.3 GHz (4.28-4.4 GHz), 5.25 GHz (5.21-5.29 GHz), and 5.68 GHz (5.62-5.75 GHz). This mode demonstrates the antenna's hexa-band performance, as seen in Figure 6. Figure 7 depicts a detailed investigation of surface current distribution at each of the six resonant frequencies. The current is centered

on the Z-shaped monopole at 2.52 GHz, and the inverted L-shaped monopole at 2.63 GHz. At 3.48 GHz, the current is largely spread over the F-shaped monopole, while at 4.3 GHz, it is scattered across the T shape monopole. At 5.25 GHz, the current is focused on the smaller T-shaped monopole, but at 5.68 GHz, it is spread across the bottom half of the patch and feed line. The suggested antenna, which operates in the L and C bands, supports 5G NR n7, n48, and IoT applications, as demonstrated by both modeling and measurement findings.

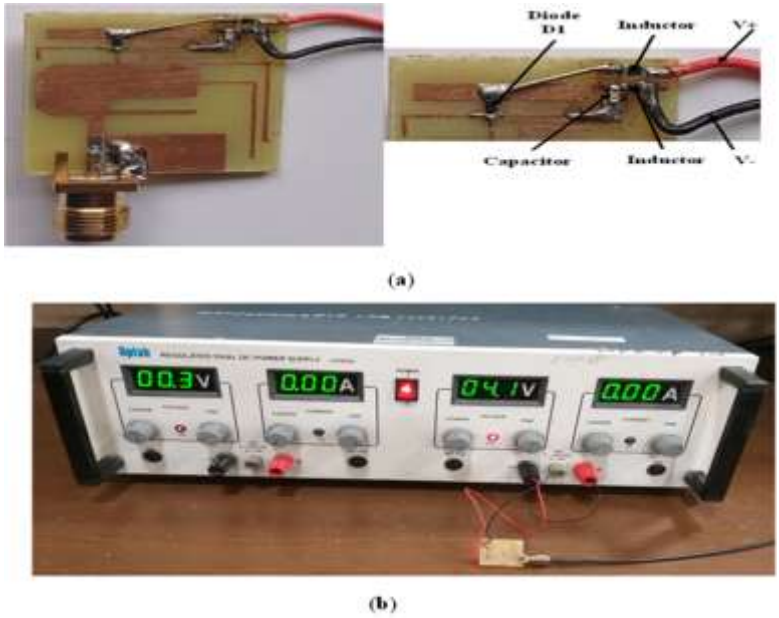

FIGURE 5. a) Physical model of the proposed antenna design, including a biasing circuit b) Experimental setup for measuring the antenna's performance

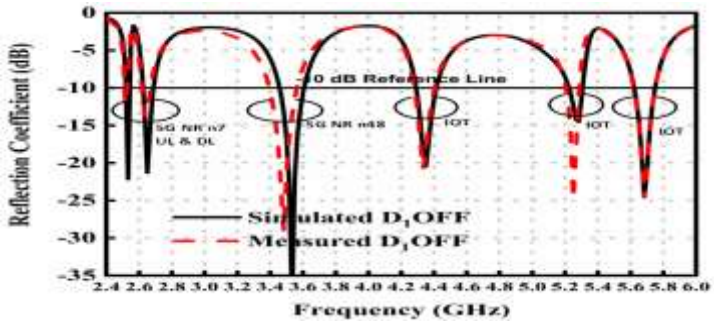

FIGURE 6. Comparison of simulated and measured S11 for Mode 1

b. Mode 2

When the PIN diode (D1) is triggered, the antenna enters Mode 2, as indicated. Figure 8 shows how the S11 characteristics of the antenna in this mode. Figure 8 shows that in this mode, the antenna exhibits triple-band behavior, with impedance bandwidths of roughly 4.31 GHz (4.25-4.38 GHz), 5.2 GHz (5.17-5.23 GHz), and 5.68 GHz (5.63-5.75 GHz). Specifically, in Mode 2, the antenna operates in the C-band, making it ideal for IoT applications

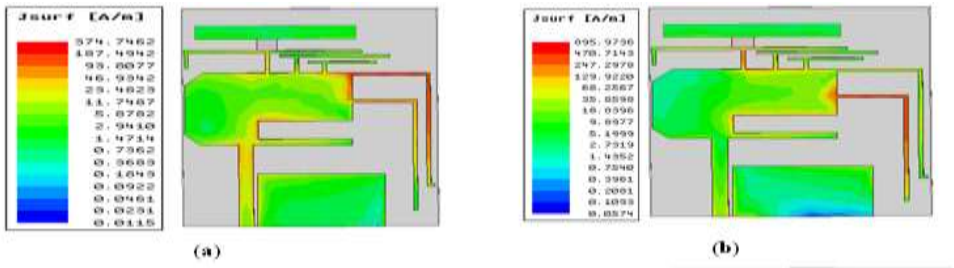

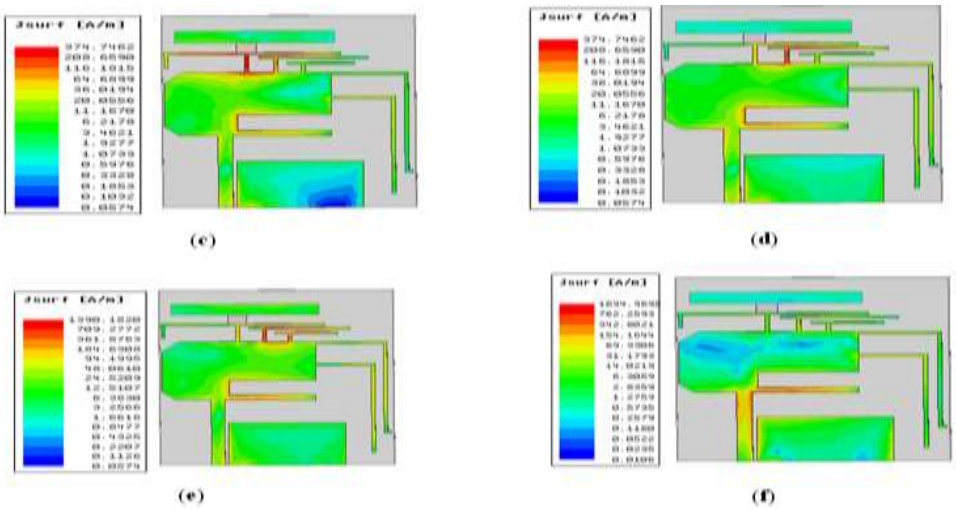

Figure 7: surface current distribution patterns at resonant frequencies of (a) 2.52 GHz, (b) 2.63 GHz, (c) 3.48 GHz, (d) 4.3 GHz, (e) 5.25 GHz, and (f) 5.68 GHz.

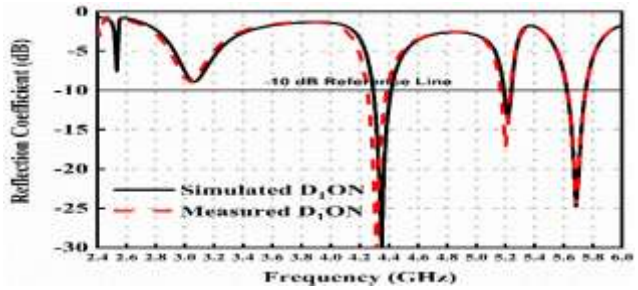

FIGURE 8. Comparison of simulated and measured S11 for Mode 2

To assess the proposed antenna's performance, simulated and measured results were compared. The investigation concentrated on important factors including impedance bandwidth, reflection coefficients (S11 in dB), and gain. The findings of this comparison are provided in Table 3. The measured and simulated results differ somewhat, which could be due to soldering errors in the PIN diodes, the DC Wires, during antenna fabrication, as well as losses imposed by the wires connecting the antenna to the measuring equipment.

TABLE III
DIFFERENT MODES AND THEIR RESPECTIVE S11, IMPEDANCE, BANDWIDTH, AND GAIN

Model	Mode	Operational frequency band (GHz)	Reflection coefficient (dB)	Bandwidth (GHz)	Bandwidth MHz	Applications	Gain (dBi)
Simulated	1	2.53	-22	2.52-2.54	20	Operates in L & C bands for 5G and IOT applications	1.6
		2.65	-21.3	2.62-2.69	70		1.9
		3.53	-38.1	3.46-3.61	150		2.84
		4.35	-20.5	4.29-4.41	120		4.2
		5.28	-14.5	5.22-5.31	90		4.9
		5.68	-24.5	5.62-5.75	130		5.8
	2	4.35	-29.8	4.29-4.42	130	Operates in C-band for IOT applications	2.85
		5.21	-13.7	5.19-5.24	50		5.46
		5.68	-24.7	5.62-5.75	130		5.98
Measured	1	2.52	-12.12	2.51-2.53	20	Operates in L & C bands for 5G and IOT applications	1
		2.63	-13.7	2.62-2.67	50		1.5
		3.48	-29.04	3.4-3.56	160		2.4
		4.3	-20.7	4.28-4.4	120		2.78
		5.25	-24.7	5.21-5.29	80		5.2
		5.68	-24.8	5.62-5.75	130		6.02
	2	4.31	-30.4	4.25-4.38	130		2.77
		5.2	-17.16	5.17-5.23	60		5.13

		5.68	-24.6	5.63-5.75	120	Operates in C-band for IOT applications	5.97

B. Efficiency

Figure 9 shows the measured total efficiency of the proposed antenna. The results show efficiencies of 90%, 78%, and 99% at 4.31 GHz, 5.2 GHz, and 5.68 GHz in the ON state (Mode 2). The values for the OFF state (Mode 1) are 58%, 76%, 77%, 89%, 86%, and 99% at 2.51 GHz, 2.63 GHz, 3.48 GHz, 4.33 GHz, 5.25 GHz, and 5.68 GHz, respectively. It is vital to note that total efficiency takes into account both the internal losses of the antenna structure and the matching losses at the input port. The definition of total efficiency η_{tot} is as follows:

$$\eta_{tot} = \eta_{rad} * (1 - |\Gamma|^2)$$

The reflection coefficient at the input port is represented by Γ, whereas the radiation efficiency is denoted by ηrad. Radiation efficiency is measured by the amount of power emitted (P_r) and lost (P_L) within the antenna structure

$$\eta_{rad} = \frac{P_r}{P_r + P_L}$$

Figure 6 & 8 shows that all antenna bands have a strong impedance match, with peak reflection coefficient values better than -16 dB. As a result, optimum total antenna efficiencies closely match the maximum radiation efficiencies. These efficiencies are 95%, 79%, and 99.5% at 4.31 GHz, 5.2 GHz, and 5.68 GHz, respectively, in the ON state (Mode 2), and 60%, 79%, 80%, 92%, 90%, and 99.5% in the OFF state (Mode 1)

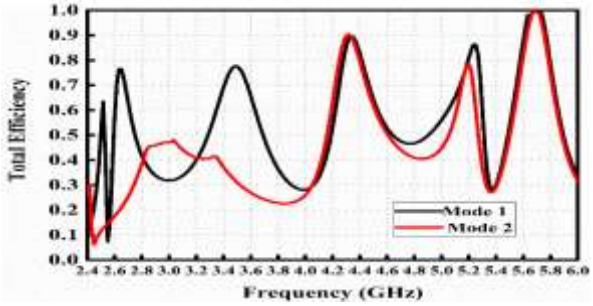

Fig. 9. Measured total efficiencies of the proposed for Mode 1 and Mode 2

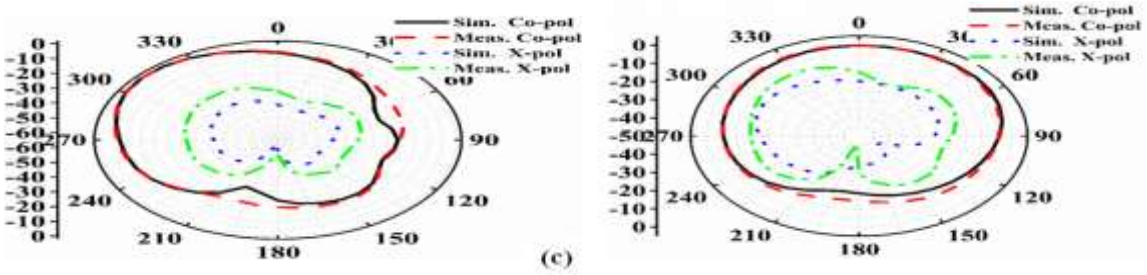

FIGURE 10: Simulated and measured radiation patterns in both E- and H-planes for Mode 1 operation at frequencies of (a) 2.54 GHz, (b) 3.45 GHz, and (c) 5.68 GHz

C. Radiation Pattern and Gain

The antenna's radiation characteristics were examined using two-dimensional E- and H-plane radiation patterns. Figure 10 shows a significant correlation between simulated and measured findings, as well as a unidirectional radiation pattern at all operational frequencies (2.54, 3.45, and 5.68 GHz). The proposed antenna's simulated gain values for 2.54, 2.64, 3.48, 4.3, 5.25, and 5.68 GHz are 1.85, 2.28, 3.46, 2.93, 5.55, and 6.26 dBi, respectively. The measured gain values at the same frequencies are 1, 1.5, 2.4, 2.78, 5.2, and 6.02 dBi, as shown in Figure 11.

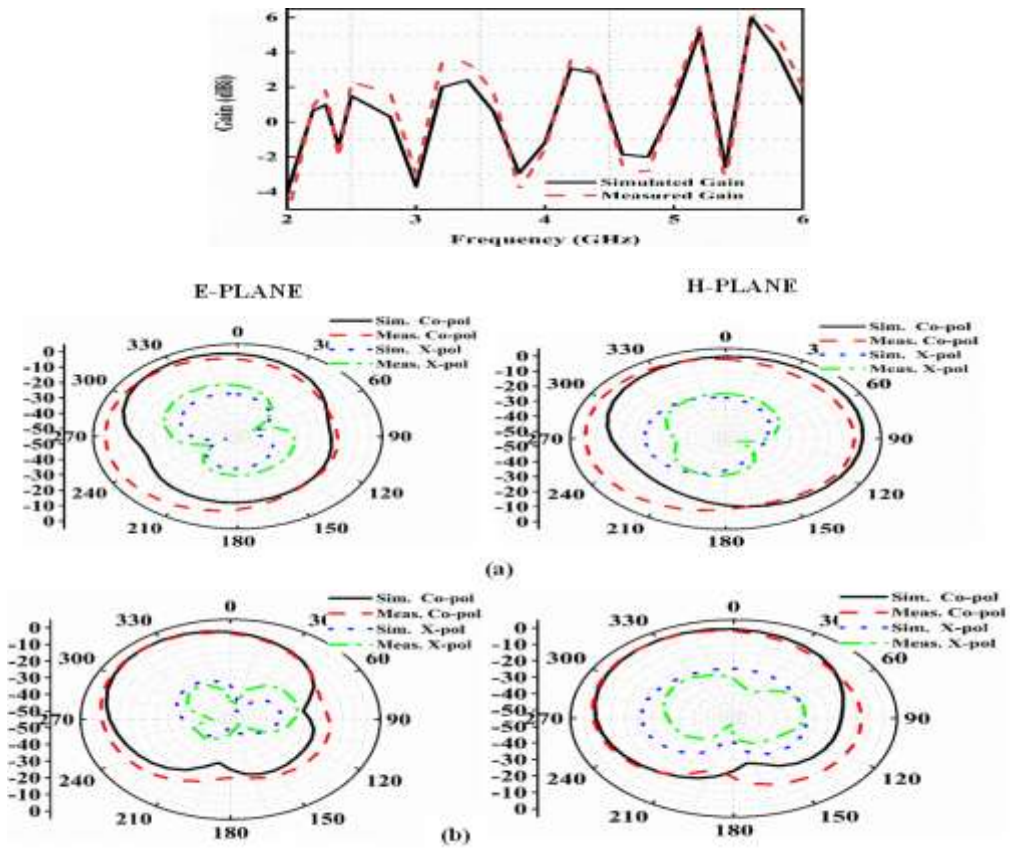

FIGURE 11. Simulated and measured gains of the proposed antenna for Mode 1

Table 4 provides a comparison of the proposed antenna with existing designs. The suggested antenna has six-band frequency reconfigurability using a single PIN diode, resulting in a simpler design and lower cost. Additionally, it has a smaller form factor than earlier designs

TABLE IV

Ref	Year	Antenna Dimensions (mm3)	Size Reduction %	No of operating Bands	Minimum Frequency Ratio	Operating Frequencies (GHz)	Frequency Reconfigurability	No of switches
[6]	2019	35 × 35 × 1.5748 1929	62	6	1.059	2.4/3.06/3.34/3.54/4.61/ 5.21	NO	NA
[9]	2021	30 × 30 × 1.6 1440	49	5	1.19	1.01/1.67/2.30/2.92 /3.48	NO	NA
[15]	2021	46 × 32 × 1.6 2355	69	5	1.16	1.8/2.1/2.6/3.5/5	YES	12
[19]	2023	70 × 60 × 1.5 6300	88	3	1.34	2.07/4.63/6.22	YES	1
Proposed work	NA	24 × 19 × 1.6 729	NA	6	1.08	2.3/2.5/3.35/4.4/5.3/5.6	YES	1

Performance comparison of the proposed antenna with state-of-the-art designs

V CONCLUSION

This paper presents a miniature multiband antenna with frequency reconfiguration capabilities. Extensive analysis and computer simulations show that the antenna is efficient at six different frequencies: 2.54/2.64/3.48/4.3/5.25/5.68 GHz. The antenna operates in the L and C bands, enabling 5G and IoT applications. Simulated gains range from 1.85 to 6.26 dBi, while measured gains range from 1 to 6.02 dBi across frequencies. The antenna design has unidirectional radiation patterns, excellent durability, low cross-polarization, consistent

radiation efficiency/gain, and better impedance matching across all operational bands. These characteristics make it an ideal candidate for integrated antennas in multiband wireless portable devices for 5G and IoT applications.

REFRENCES

[1] Balanis, C. A., Antenna Theory Analysis and Design, 4th edition, John Wiley & Sons, 2016.

[2] A. Rashidy, A. M, and M. A, "Compact Planar Multiband Antennas for Mobile Applications', Advancement in Microstrip Antennas with Recent Applications," InTech, Mar 2013. https://doi.org/10.5772/52053

[3] Nasimuddin, Z. N. Chen and X. Qing, "Dual-Band Circularly Polarized S-Shaped Slotted Patch Antenna With a Small Frequency-Ratio," IEEE Transactions on Antennas and Propagation, vol. 58, no. 6, pp. 2112-2115, June 2010. https://doi.org/10.1109/TAP.2010.2046851

[4] S. Kumar, B. K. Kanaujia, M. K. Khandelwal and A. K. Gautam, "Stacked dual-band circularly polarized microstrip antenna with small frequency ratio", Microw. Opt. Technol. Lett., vol. 56, no. 8, pp. 1933-1937, Aug. 2014. https://doi.org/10.1002/mop.28482

[5] Chaurasia, P., Kanaujia, B., Dwari, S., & Khandelwal, M," Penta-band microstrip patch antenna with small frequency ratios using metamaterial for wireless applications," International Journal of Microwave and Wireless Technologies, vol.10, no. 8, pp. 968-977, 2018. https://doi.org/10.1017/S1759078718000570

[6] Praveen Chaurasia, Binod Kumar Kanaujia, Santanu Dwari & Mukesh Kumar Khandelwal," Metamaterial based circularly polarized hexa-band patch antenna with small frequency ratios for multiple wireless applications," Journal of Electromagnetic Waves and Applications, vol. 33, no. 4, pp. 520-540, 2019. https://doi.org/10.1080/09205071.2018.1561330

[7] C. -X. Mao, S. Gao, Y. Wang and B. Sanz-Izquierdo, "A Novel Multiband Directional Antenna for Wireless Communications," IEEE Antennas and Wireless Propagation Letters, vol. 16, pp. 1217-1220, 2017. https://doi.org/10.1109/LAWP.2016.2628715

[8] Antara Ghosal, Sisir Kumar Das, Annapurna Das, "Multifrequency rectangular microstrip antenna with array of L-slots, AEU - International Journal of Electronics and Communications," vol. 111, 2019. https://doi.org/10.1016/j.aeue.2019.152890

[9] Daniel, R. Samson. "A CPW-fed rectangular nested loop antenna for penta band wireless applications," AEU - International Journal of Electronics and Communications, vol. 139 2021. https://doi.org/10.1016/j.aeue.2021.153891

[10] Chaurasia, Praveen & Kanaujia, Binod & Dwari, Santanu & Khandelwal, Mukesh, "Antenna with hexa-band capabilities for multiple wireless applications," Progress in Electromagnetics Research C, vol. 82, pp. 109-122, 2018.https://doi.org/10.2528/PIERC17120602.

[11] Songnan Yang, Chunna Zhang, H. K. Pan, A. E. Fathy and V. K. Nair, "Frequency-Reconfigurable Antennas for Multiradio Wireless Platforms," IEEE Microwave Magazine, vol. 10, no. 1, pp. 66-83, February 2009, https://doi.org/10.1109/MMM.2008.930677.

[12] Rayirathil Kadavath Athira Mohan, and Kanagasabapathi Girirajan Padmasine, "A Review on Materials and Reconfigurable Antenna Techniques for Wireless Communications: 5G and IoT Applications," Progress in Electromagnetics Research B, Vol. 97, 91-114, 2022.https://doi.org/10.2528/PIERB22092005

[13] Komulainen, Mikko, Palukuru, Vamsi Krishna and Jantunen, Heli. "Frequency-Tunable Dual-Band Planar Inverted-F Antenna Based on a Switchable Parasitic Antenna Element" Frequenz, vol. 61, no. 9-10, pp. 207-212, 2007. https://doi.org/10.1515/FREQ.2007.61.9-10.207

[14] Ghaffar, A, Li, XJ, Awan, WA, Nazeri, AH, Hussain, N, Seet, B-C," Compact multiband multimode frequency reconfigurable antenna for heterogeneous wireless applications," Int J RF Microw Comput Aided Eng. 2021. https://doi.org/10.1002/mmce.22659

[15] I. Ahmad et al., "A Pentaband Compound Reconfigurable Antenna for 5G and Multi-Standard Sub-6GHz Wireless Applications," Electronics, vol. 10, no. 20, pp. 2526, Oct. 2021. https://doi.org/10.3390/electronics10202526.

[16] Adnan Ghaffar, Ahsan Altaf, Aayush Aneja, Xue Jun Li, Salahuddin Khan, Mohammad Alibakhshikenari, Francisco Flalcone, Ernesto Limiti, "A Frequency Reconfigurable Compact Planar Inverted-F Antenna for Portable Devices", International Journal of Antennas and Propagation, vol. 2022, Article ID 7239608, 2022. https://doi.org/10.1155/2022/7239608

[17] Sreelakshmi, K., Rao, G.S," Reconfigurable Quad-Band Antenna for Wireless Communication," Journal of Electr. Eng. Technol, vol. 15, pp. 2239–2249, 2020. https://doi.org/10.1007/s42835-020-00492-9

[18] Omaima Benkhadda, Mohamed Saih, Abdelati Reha, Sarosh Ahmad, Kebir Chaji, Harbinder Singh, and Ahmed Jamal Abdullah Al-Gburi, "A Miniaturized Reconfigurable Antenna for Modern Wireless Applications with Broadband and Multi-Band Capabilities," Progress in Electromagnetics Research M, Vol. 127, 93-101, 2024.https://doi.org/10.2528/PIERM24042801

[19] Sakkas, A., Oikonomou, V., Mystridis, G., Christofilakis, V., Tatsis, G., Baldoumas, G., Tritiakis, V., & Chronopoulos, S. K. (2023). A Frequency-Selective Reconfigurable Antenna for Wireless Applications in the S and C Bands. Sensors, 23(21), 8912. https://doi.org/10.3390/s23218912